ISSN 2035-1755
Vol.1 No.3
May 2009

International Review of Chemical Engineering

Rapid Communications

(IRECHE)

Contents:

Manuscript received and revised June 2008, accepted July 2008

Analysis of the Response of Thermal Sensors in Adsorption Microcalorimetry

V Garcia-Cuello [1], J C Moreno-Piraján [1,] *, L Giraldo-Gutiérrez [2] , K Sapag[3]

Abstract – *Three different designs for adsorption calorimeters are presented, which use sensors based on the Seebeck effect. The noises of signals with respect to the baseline are evaluated on each one of the builded equipment and the detection limit of the thermal effects is expressed in µWatt. It was determined that the different designs and working conditions affect the baseline noise and the detection limit. Values of the noise in the baseline are between ± 100 µV and ± 0,5 µV and between 887,2 and 24 µWatt. These values allow making measures in the solid-gas interphase with very good precision.*

Keywords*: Adsorption calorimeter, noise baseline, heat flow, Seebeck effect*

I. Introduction

When a calorimetric project is undertaken, it is necessary to choose the method. The factors that must be considered in the selection of a calorimetric method are numerous.

One of the most important factors to be considered is the required precision. The required effort increases exponentially with the desired high precision. Some calorimetric measurements near room temperature can be made with 1% of precision using a Dewar bottle of common use in the laboratory and a very simple instrumentation. Precision measurements of up to 0,1%, require an increase of at least one or two orders of magnitude in the efforts to reach this precision level.

Precision measurements of up to 0,01% are usually non practical for some calorimeters, although in some cases with many efforts this level of precision can be obtained. At extreme temperatures or other conditions, the difficulties to maintain this precision near 1% can be as great as to maintain it in the order of 0,01% at room temperature.

Another important factor related to the required precision is whether relative or absolute measurements will be made. If the required precision is not very high, as the precision obtained in calorimetric measurements published on certain materials, then the use of a reference material can be advantageous for "calibrating" a less complex calorimeter.

The physical properties of the sample and the thermal properties to be measured usually have a considerable influence on the selection method and calorimetric design. The temperature and the involved precision rank in the measures are important, as well as the amount of sample available. If only some milliliters of solid or liquid sample are available and it is required to realize a great number of measurements, the use of the "drop" method offers a greater simplicity. This method is very useful to obtain heat capacity values if this one does not change quickly with the temperature [1-26].

If the measurements involve small heat variations, it is very advantageous to use the "twin calorimeter" system to decrease the errors introduced by uncertainties due to loss of heat. In microcalorimetry, the twin calorimeter frequently is therefore used.

Other important factors that must be considered in this exciting and delicate task of designing and constructing calorimeters, are briefly enumerated below:

Rank of work temperature
Duration of the experiment.
Costs of the required apparatus.
Availability of the elements and the personnel required.
Mechanical aspects.
Electrical aspects

Within these aspects it is important to consider the system of thermal registry that is going to be used; in the high precision calorimeters as those described in this investigation, those based on the Seebeck effect, i.e. thermopiles, are used as thermal sensors [25].

I.1 Thermopiles Theory

An important aspect in the design calorimetric is the choice of sensor. In this study we have used thermopiles operating under the Seebeck effect. Several researches have made a clear description of this phenomenon thermoelectric, but we in this part we have taken the developers authors of the reference [26].

The Seebeck effect

If two semiconductors a and b are joined together at the hot point and a temperature difference ΔT is maintained between this point and the cold point (see Fig. 1 (a)), then an open circuit voltage ΔV is developed between the leads at the cold point. This effect, called the Seebeck effect after its discoverer T. J. Seebeck (1770 - 1831), can be mathematically expressed by

$$\Delta V = \alpha_s \Delta T \tag{1}$$

Where αs is the Seebeck coefficient expressed in V/K (or more commonly in μV/K). It was found that only a combination of two different materials, a so-called thermocouple, exhibits the Seebeck effect. For two leads of the same material no Seebeck effect is shown, for reasons of symmetry. It is, however, somehow present because the Seebeck effect is a bulk property and does not depend on a specific

arrangement of the leads or the material, nor on a specific way of joining them. This bulk property can be expressed as

$$VE_F / q = \alpha_s VT \qquad (2)$$

Where EF is the Fermi energy (and EF/q = ΦF is the electrochemical potential), and where the Seebeck coefficient αs depends, among other things, upon the chemical composition of the material and upon the temperature.

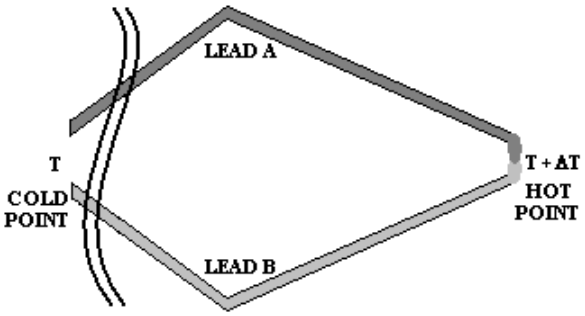

Fig 1. (a) Seebeck Effect.

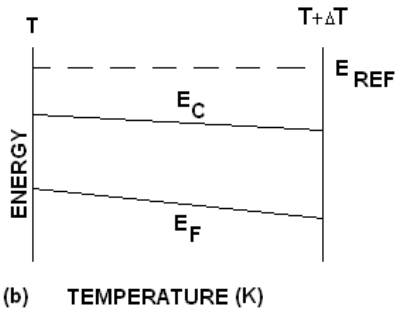

Fig 1. (b) Variation of EF due to ΔT. (with permission of Elsevier) [26]

The Seebeck coefficient of, for example, silicon, can be derived by setting αs as (see Fig. 1(b))(with permission of Elsevier)[26]

$$\alpha_s = \frac{d}{q\,dT}\left(E_F\right) \qquad (3)$$

For non-degenerate silicon the Seebeck coefficient may be approximated by using simple Maxwell-Boltzmann statistics. Three main effects are present.

First, with increasing temperature the silicon becomes more intrinsic:

$$\frac{d}{q\,dT}\left(E_F\right)_{E_C - E_F} = -\frac{\kappa}{q}\left(\ln\left(N_c / n\right) + \frac{3}{2}\right) \qquad (4)$$

where Ec is the conduction-band edge energy, Nc the conduction-band density of states, n the electron density (fixed by the doping concentration) nd and k the Boltzmann constant.

Secondly, with increasing temperature the charge carriers have a higher average velocity, leading to charge build-up on the cold side of the silicon.

Moreover, the scattering of charge carriers is usually energy (and thus temperature) dependent, likewise leading to charge build-up on the cold or hot side of the silicon, depending on whether the hot carriers can move more freely than the cold carriers or are 'trapped' by increased scattering:

$$\frac{d}{q\,dT}\left(E_F\right)\Big|_{\tau} = -\frac{\kappa}{q}\left(1+s\right) \tag{5}$$

where τ is the relaxation time (mean free time between collisions) and s is the exponent describing the relation between τ and the charge-carrier energy.

Finally, the temperature difference in the silicon causes a net flow of phonons from hot to cold. In a certain temperature region (10 to 500 K) and for non-degenerate silicon, a transfer of momentum from acoustic phonons to the charge carriers can occur. As there is a net phonon momentum directed from hot to cold, this will drag the charge carriers towards the cold side of the silicon. This effect may be represented by:

$$\frac{d}{q\,dT}\left(E_F\right)\Big|_{\phi_n} = -\frac{\kappa}{q}\phi_n \tag{6}$$

in which Φn denotes the phonon drag effect. In sum, the total Seebeck coefficient in non-degenerate silicon becomes:

$$\alpha_s = -\frac{\kappa}{q}\left\{\ln\left(N_c/n\right)+\frac{5}{2}+s_n+\phi_n\right\} \quad n-type \tag{7}$$

$$\alpha_s = +\frac{\kappa}{q}\left\{\ln\left(N_v/p\right)+\frac{5}{2}+s_p+\phi_p\right\} \quad p-type \tag{8}$$

where s is of the order -1 to 2, and where he phonon-drag contribution Φ ranges from 0, for highly-doped silicon, to approximately 5, for low-doped silicon, at 300 K, while Φ ranges from 0, for highly-doped silicon, to 100, for low-doped silicon, at low temperature (100K). In practice, the Seebeck coefficient may be approximated, for the range of interest for use in sensors and at room temperature, as a function of electrical resistivity:

$$\alpha_s = \frac{m\kappa}{q}\ln\left(p/p_o\right) \tag{9}$$

II. Experimental Section

II.1.1. Design Criteria

The desired equilibrium information for adsorbed mixtures is the pressure and composition of the gas phase above the adsorbent for a given loading, as well as the heat evolved for differential increases in the loading. Because we consider direct calorimetric measurements of differential heats to be more reliable than differentiation of isotherms at various temperatures, the instrument was built around a Tian-Calvet calorimeter. Practical limitations on the ability to integrate the heat flow in the calorimeter as a function of time required that equilibrium be established in 15 min or less. The necessity of establishing equilibrium within 15 min of changing the sample loading placed a stringent limitation on the design. The major limitation for the attainment of adsorption equilibrium is gas-phase mixing in the region above the sample. On the basis of a typical gas-phase diffusion coefficient of 0.1 cm2s-1, a tube length of even 10 cm will result in mixing times of 1000 s. This imposes significant challenges on the instrument design. While imposed circulation would alleviate this problem, forced flow would also complicate the design of the calorimeter because of convective heat losses. The maximum distance within our equipment (from the bottom of the sample cell to the diaphragm of the pressure transducer) was approximately 10 cm. The pressure transducer was chosen for its small dead volume. The leak valve for the composition measurements was welded directly on the top of the cell to minimize the dimensions of the apparatus. These design criteria could only be met by a custom-made calorimeter. In general this calorimeter is based in literature design and experience of our laboratory [27, 28].

II.1.2. Practical Calorimeter

In the idealized calorimeter, the temperature of the gas in the sample loop decreases upon expansion while the temperature of the gas in the sample cell increases as it is compressed by the incoming gas. In the absence of adsorption, heat is absorbed by the dosing loop and heat is liberated by the sample cell until the pressures equalize and the temperature returns to T_0. For a perfect gas, the two effects cancel because the enthalpy of a perfect gas is a function only of temperature.

Our design is a modification of the idealized calorimeter in which only the sample cell is placed in the calorimeter. Because the dosing loop and valve are external to the calorimeter, adding a dose of gas to the sample cell generates an exothermic heat of compression in the sample cell which is not cancelled by absorption of heat in the dosing loop. The spurious heat of compression calculated from eq 21 is subtracted from the total heat registered by the calorimeter in order to obtain the heat of adsorption.

II.1.3. Description of Model I Microcalorimeter

A diagram of the calorimeter apparatus is shown in Figure 2; the components are described in Table 1. A picture of the sample cell and its connections is shown in Figure 3. The stainless steel cube is the sample cell for the adsorbent and adsorbate. The use of stainless steel to maximize heat conduction through the top of the cell is a crucial element of the design of the heat conduction type. The stainless cube is surrounded on all four sides and on the bottom by square thermal flow meters (shown in the picture) obtained from the Melcor Corporation™. Each thermopile is a 40x40x2 mm ceramic plate with about 240 embedded thermocouples for detecting temperature differences across the plate.

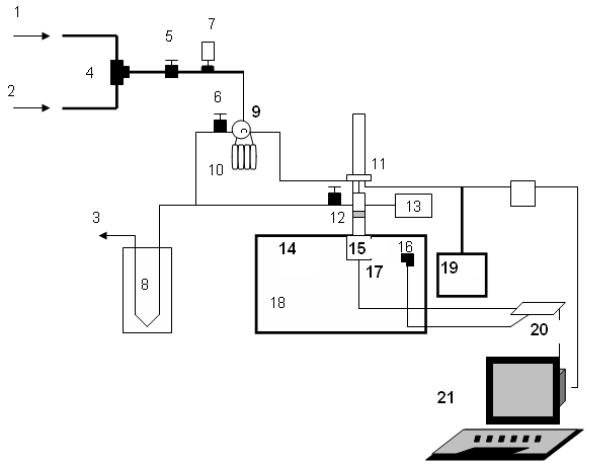

Fig 2. Schematic diagram of microcalorimeter system and auxiliary equipment.

TABLE I
COMPONENTS OF MICROCALORIMETER. KEY TO FIGURE 1.

No.	Description	Model No.
1	Gas 1 inlet	
2	Gas 2 inlet	
3	To vacuum pump	
4	Three-way valve	
5	Inlet valve to the dosing loop	
6	Outlet valve from the dosing loop	
7	Pressure transducer for the dosing loop	Teledyne™
8	Liquid nitrogen trap	
9	Valco six-way valve	
10	Calibrated dosing loop (5 cm^3)	
11	Variable leak valve	Granville-Phillips 203™
12	Cell outlet valve	
13	Pressure transducer for the cell	Edwards™, 655 and 622

14	Reference cell	
15	Calorimeter cell	
16	K-type thermocouple	
17	Thermopiles	Tellurex Corporation™
18	Heat sink (aluminium block)	
19	Turbo pump	Pfeiffer ™
20	Data acquisition board	
21	Computer	

The signal from these thermopiles was input to a system for the data acquisition through a computer.

The sample cell slides into cubical holes cut into an aluminum block (10x13x8 cm, mass 1 kg). A silicone based heat-sink compound was used to ensure good thermal contact between the Al block and the thermopiles and between the thermopiles and the stainless steel.

The cubical stainless steel cell shown in Figure 3 on the top was inserted into a Cajon fitting, which provides a vacuum seal by compression of a Viton O-ring. The Cajon fitting connects to a custom-made T connection onto which are welded the leak valve, the pressure head, the connection to vacuum, and the 0.01-in. bore tube from the dosing loop. The leak valve is connected through a 1/4-in.-o.d. stainless-steel tube; the pressure head is connected through a 1/4-in. δ NPT fitting; the valve that opens to vacuum is connected through a 1/4-in. VCR fitting. The pressure head was chosen for its small dead space (2.0 cm3). The total dead space is 17.8 cm3 for the (empty) sample cell, the dead space inside the pressure head and the lines to vacuum, the dosing loop, and the RGA leak valve.

Gas was introduced to the sample cell from the dosing loop using a six-port Valco sampling valve connected to a small bore (0.01-in.-i.d.) tube. The small diameter of the tube prevents back mixing of the mixture into the dosing loop.

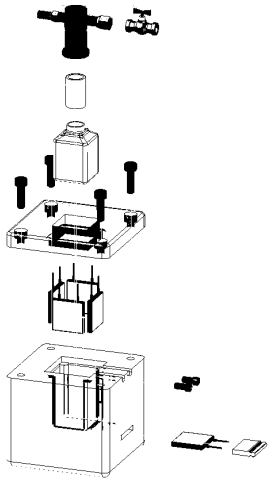

Fig 3. Picture of the stainless steel sample cell and connections to the pressure head, vacuum line, dosing loop and leak valve. The stainless steel sample cell is surrounded by thermopiles set into an aluminum heat sink.

This tube enters the T-shaped connector from the back (the welded connection does not appear on Figure 3) and extends downward, with the opening 5 cm above the bottom of the sample cell. Two small metal cylinders with a Viton O-ring between them were inserted in the NPT connection to the pressure head to make a vacuum seal.

The adsorbent was covered with a 1.5 cm layer of glass chips to minimize heat loss through the top of the cell and regenerated in situ.

II.1.4. Description of Model II Microcalorimeter.

Figure 4 shows a complete exploded view of the adsorption calorimeter built here, which is not very common and has not been considered in the literature.

A detailed view from the inner part of the equipment toward the exterior of the calorimeter is shown. In the diagram, part number 1 corresponds to the calorimetric cells made of stainless steel (sample and reference), which are embedded inside a large block (also divided in two parts) in stainless steel , parts 4a and 4b, which acts as deposit of the thermostatic liquid; due to its thermal diffusion coefficient, this set allows the rapid heat conduction towards the surrounding of the calorimeter. The calorimeter cells are fixed to the block through part 2, constructed in stainless steel; the sensor with thermopiles is shown in the figure as part 3. The whole set is placed inside a nylon block (not shown in the Figure 4) to isolate it from the surroundings and to allow the rapid stabilization of the temperature. The calorimetric cell have external measures are 36mm in the base by 95 mm in height. Nevertheless inside the volume is of 5 mL due to its tubular structure.

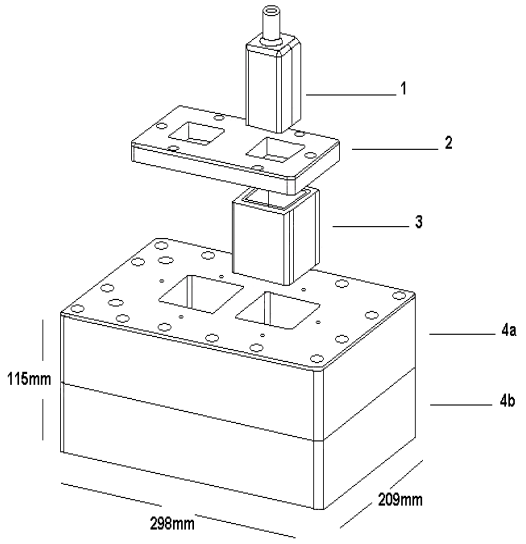

Fig 4. Exploded view of the adsorption microcalorimeter.

At the top part of the block and the profile where the thermopiles and the calorimetric cells are placed. The thermal effects are sensed through ten thermopiles (five for each cell), trademark Melcor Corporation™, connected in series to increase the sensitivity of the microcalorimeter. These thermo elements, due to Seebeck effect, generate a voltage signal which is proportional to the heat flow produced in the cell.

This thermoelectric potential is recorded by means of a $6^{1/2}$ digits Aligent multimeter, model 34349, and is connected to a computer through an RS-232 interfase.

Figure 4 shows the microcalorimeter designed in this work connected to the adsorption system constructed specially for this equipment in stainless steel to allow for the simultaneous measurement of the heat of adsorption and the isotherm. The connection is through two pressure transducers, one in the range of high pressure (1000 Torr), and the other in the range of low pressure (10 Torr). The transducers are a trademark Edwards. The station is complemented by two vacuum pumps, a rotating one and an ultra high vacuum one, and an oven for degassing the sample, with a temperature controller. The adsorption system is connected to a system of data capture developed in our laboratory [27,28].

II.1.4.1. Electric calibration of the adsorption microcalorimeter.

In order to establish the correct functioning of the micro calorimeter, which is then connected to the volumetric adsorption unit, the sensitivity is evaluated determining the calorimeter constant.

The calibration constant reports the voltage generated by the calorimeter when a heat flow is emitted from inside the microcalorimetric cell.

There are two methods to determine the calibration constant K:

● Determination of the calibration constant by application of electric power.

This method is based on the dispersion of an electric work ,W_e, through an electric resistor through which an electric current, i, passes during a certain amount of time t; in the micro calorimeter a voltage, V_t, is generated and this is measured.

According to Steckler, Goldberg, Tewari and Buckley [29,30] the micro calorimeter calibration constant, K, is given by:

$$K = \frac{We}{\int V_t dt} = \frac{V_c it}{\int V_t dt} \qquad (10)$$

Where V_c is the voltage provided to the resistor, i is the current that passes through it and t is the time expressed in seconds.

● Determination of the constant by the stationary method

This is an alternate method to the one above, which is useful to compare and evaluate whether the constant K assessed by the above method is correct. The method consists in applying a constant voltage, V_c, through the micro calorimeter electric resistor until the voltage generated by the calorimeter, V_t, reaches the condition of stationary state. Under these conditions, K is given by:

$$K = \left(\frac{V_c i}{V_t} \right)_{stationary} \qquad (11)$$

II.1.5. Description of Model III Microcalorimeter.

In this equipment the thermal gradient calorimeter transfers all the heat developed in a reaction to its surrounding heat sink at constant temperature. This equipment uses a 3D sensor type. Transient as well as steady state energy releases may be measured.

The walls are composed of a thin high temperature thermopile structure containing thousands of junctions which are in thermal contact with one wall surface, and the other set is in contact with the opposite surface. As heat flows through the walls a temperature difference is established between both sets of thermopile junctions, thus generating a voltage wich is directly proportional to the heat flow. The large numbers of thermopiles develop extreme sensitivity under diminute heat flows. See Figure 5.

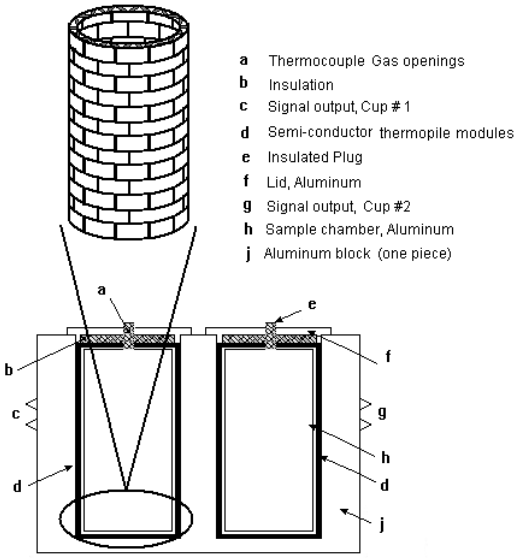

Fig 5. Adsorption Microcalorimeter with 3D sensors type.

III. Discussion and Conclusions

A thermoelectrial registry with each one of the calorimeters constructed for this investigation is obtained, with the aim of establishing their detection limits and sensitivity.

Figure 6 shows a potentiogram elaborated with the equipment in Figure 3 (Model I); a zoom is applied to the potentiogram interval between 2000 and 2550 seconds to evaluate the noise in the baseline potential signal obtained in this equipment, with a value of ± 15 μV and 887μW of power in the heat flow measurement, under operational conditions. These results in the thermopiles answer, the test design, are within levels that allow undertaking solid-gas interphase studies with a reasonable precision. The thermogram shows that in approximately half an hour in a measurement of electrical calibration the thermopiles signal becomes stabilized.

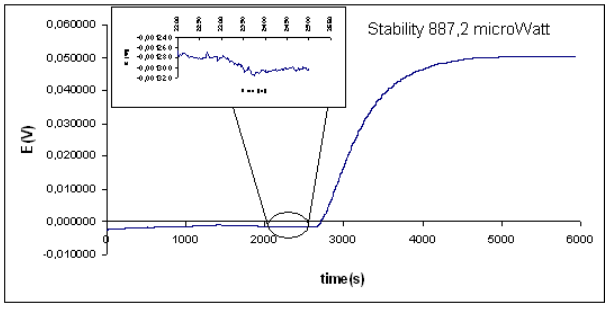

Fig 6. Potenciogram obtain with calorimeter Model I. Noise in the stability line is ± 15 μV and range of heat flow measurement of 887,2 μWatt.

A more detailed study was made on the noise resulting in the baseline signal for the calorimeter builded and illustrated in Figure 4 (MODEL II). Figure 7 shows a section of the sensors answer obtained from a cell; the noise level of the cells is 100± μV. This level is greater than that obtained for Model I microcalorimeter, but it must be emphasized that this determination is performed without a strict temperature control, and with another type of sensor disposition, since in the first design there are only 5 sensors, whereas in this second model there are altogether 10 thermopiles connected in serial and contraposition.

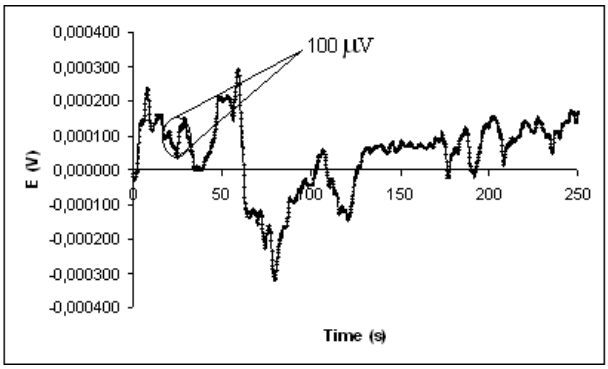

Fig 7. Potenciogram obtain with calorimeter Model II. Noise in the stability line is ±100 µV.

When measuring the signal on the same calorimeter once assembled with the two cells (test and reference) and with an ice-water bath, the noise level decreases to ± 50 µV, result obtained during a stabilization time of 4 hours in the output signal of the equipment.

When the equipment was stabilized at a temperature of 18°C ± 0,001, as shown in Figure 8, the noise surprising reaches a low value of ± 5 µV, an excellent value compared to those reached in our laboratory and to those reported in literature.

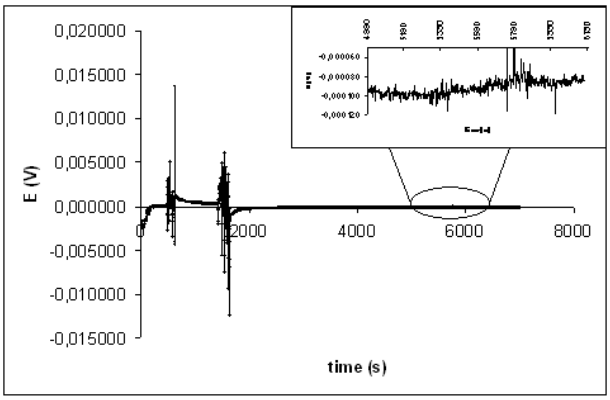

Fig 8. Potenciogram obtain with Calorimeter Model II. Noise in the stability line is ± 5 µV.

The difference with respect to the result of ± 50 µV obtained with the ice-water bath is explainable, because the evaporation control system is complex and this is reflected in the output signal noise in the sensors.

Later, a study under optimal conditions was made with this equipment where the temperature was controlled during the signal capture and a noise level of ± 0.5 µV was obtained, as well as a value of 481 µW as the range of measurement for the heat flow, values that really show a great contribution of this Calvet type calorimeter design, as shown in figure 9.

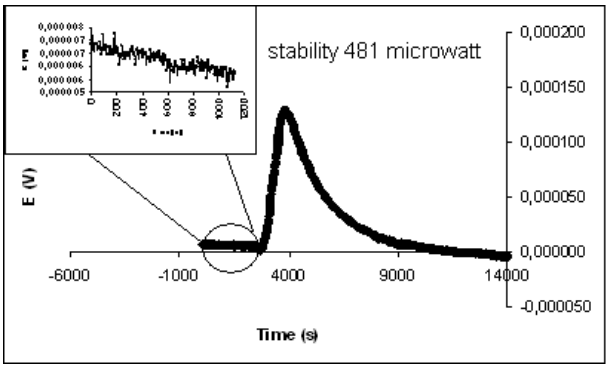

Fig 9. Potenciogram obtain with calorimeter Model II. Noise in the stability line is ± 0.50 μV and the range of heat flow measurement is of 481 μWatt.

Finally the Model III Microcalorimeter of Figure 5 was designed and constructed; as it can be seen the baseline noise signal, under operational conditions, is ±0.5 μV and 24 μW. These results shows that the change in the sensors design is fundamental and cause an impact on the heat flow measurement range, value that is excellent for the type of studies that usually are performed with this type of equipment. As shown in figure 10, this calorimeter uses 3D sensors that are more accurate than those used in previous models in determining any thermal effect ,since in this one the calorimetric cells of measurement rolls in all 3 dimensions. It is necessary to point out that with this equipment a heat detection limit was obtained far beyond that reported in specialized literature, making of this equipment a novel contribution.

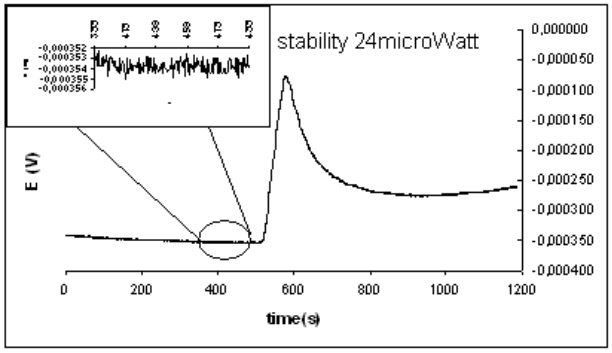

Fig 10. Potenciogram obtain with Model III calorimeter. Noise in the stability line is ± 0.50 μV and the range of heat flow measurement is of 24 μWatt.

Thus, three equipment of very good operation and thermal characteristics was designed and builded which can to be used for studies in the solid-gas interphase and additionally, it is worth to say, at a reasonable cost in comparison with the commercial ones.

Acknowledgements

The authors thank the Departments of Chemistry of Universidad Nacional de Colombia, Universidad de Los Andes (Colombia) and Universidad Nacional de San Luis (Argentina) and the Master Agreement established between these institutions. Special gratitude is due to Fondo Especial de Investigaciones de la Facultad de Ciencias de la Universidad de Los Andes (Colombia) for its partial financing. Prof. Moreno, thanks Universidad Nacional de San Luis, UNSL (Argentina) for a Visiting Professor Fellowship at this University.

References

[1] S.J. Sircar, Excess properties and thermodynamics of multicomponent gas adsorption. *J.Chem.Soc. Faraday Trans. 81 (1985), 1527-1540.*

[2] J.A. Dunne, Rao, M.; Sircar. ; Gorte, R.J.; Myers, A.L. Calorimetric Heats of Adsorption and Adsorption Isotherms. 3. Mixtures of CH_4 and C_2H_6 in Silicalite and Mixtures of CO_2 and C_2H_6 in NaX. *Langmuir 13 (1997) 4333-4341.*

[3] Hill, T.L. Statistical Mechanics of Adsorption. V. Thermodynamics and Heat of Adsorption. *J.Chem.Phys. 17 (1949) 520-535.*

[4] J.A. Duna, R. Mariawala, M. Rao, S.Sircar, R.J. Gorte, A.L. Myers, Calorimetric Heats of Adsorption and Adsorption Isotherms. 1. O_2, N_2, Ar, CO_2, CH_4, C_2H_6, and SF_6 on Silicalite**.** *Langmuir, 12 (1996) 5888-5895.*

[5] Handy, T.L.; Sharma,S.B.; Spiewak, B.E; Dumesik, J.A. A Tian-Calvet heat-flux microcalorimeter for measurement of differential heats of adsorption**.** *Meas.Sci.Technol., 4 (1993) 1350-1356.*

[6] G.C. M. Meijer, Thermal sensors base don transistors. *Sens. Actuators, 10 (1996) 117-139.*

[7] G.D. Nieveld, Thermopiles fabricated using silicon planar technology, *Sens. Actuators, 3 (1983) 179 – 183.*

[8] P.M. Sarro, van herwaarden, A.W. Silicon Cantilever beams fabricated by electrochemically controlled etching (ECE) for sensor applications, *J. Electrochem. Soc., 133 (1986) 1724–1729.*

[9] H.N. Norton, In *Sensor and Analyzer Handbook*; (Prentice-Hall: New Jersey, 1982).

[10] H.N. Norton, In *Handbook of Transducers for Electronic Measuring Systems* (Prentice-Hall: New Jersey, 1969).

[11] H.K.P. Neubert, In *Instrument Transducers* (Clarendon Press: Oxford, 1975).

[12] P.H. Mansfield, In *Electrical Transducers for Industrial Measurement* (Butterworths: London, 1973).

[13] P.H Sydenham., In *Handbook of Measurement Science* (Ed.; Wiley: Chichester, 1983; Volume 2).

[14] F. Bulnes, A.J Ramírez-Pastor.; G. Zgrablich, Scaling Behavior of Adsorption on Patchwise Bivariate Surfaces. *Langmuir, 23 (2007) 1264-1270.*

[15] R.R. Heikes, W. Ure, In *Thermoelectricity: Science and Engineering* (Interscience Publishers: New York, 1961).

[16] P.M. Sarro, van Heraarden, A.W. Inhomogeneity effects in silicon thermopiles, In Proc. 2nd *Sensors and Actuators Symp., Enschede, The Netherlands, 1 (1984) 129–135.*

[17] L. Onsager, Reciprocal relations in irreversible process *II, Phys. Rev. 37 (1931) 2265-2274.*

[18] F.J Blatt, P.A. Schroeder, C.L. Foiles, D. Greig, In *Thermoelectric Power of Metals* (Plenum Press: New York, 1976).

[19] Barnard, R.D. In *Thermoelectricity* in Metals and Alloys (Taylor and Francis Ltd.: London, 1972).

[20]. T.J. Quinn, In *Temperature*; (Academic Press: London, 1983).

[21] H.J. Goldsmid, In *Applications of Thermoelectricity* (Butler and Tanner Ltd.: London, 1960).

[22] T.H. Geballe, G.W. Hull, Seebeck effect in silicon, *Phys. Rev. 98 (1955) 940–947.*

[23] H.G. Kerkhoff, G.C. M. Meijer, An integrated electrothermal amplitude detector using the Seebeck effect, *In Proc. ESSCIRC, Southampton, U. K., 1979; 31-33.*

[24] W. Hemminger, G. Höhne, In *Grundlagen der Kalorimetrie, Verlag Chemie: Weinheim*, (Germany, 1979).

[25] W. Langer, *Ein Wärmeleitungs-Gasdruck-Kalorimeter und die simultane Messung von Isothermen und Wärmen der Adsorption von N_2 an SiO_2,* (Dissertation, FB Chemie-Biologie, Universität Siegen, 1994).

[26] Van Herwaarden, P.M. Sarro, Thermal sensors based on the Seebeck effect, *Sens. Actuators A, 10 (1986) 321-346.*

[27] J.C. Moreno, L. Giraldo, Setups for simultaneous measurement of isotherms and adsorption heats**.** *Rev. Sci. Instrum., 76 (2005) 1-8.*

[28] M. Huertemendia, L. Giraldo, D. Parra, J.C. Moreno, Adsorption Microcalorimeter and its Software: Design for the Establishment of Parameters Corresponding to Different Models of Adsorption Isotherms. *Inst. Sc. & Tech., 33 (2005) 645-660*

[29] D.K. Steckler, R.N.Golderg, Y.B. Tewari, T.J. Buckley, High precision microcalorimetry: apparatus, procesures, and biochemical applications. *J. Res. Natl. Bur. Stand. 91 (1986) 113-121.*

[30] G. Kegeles, The Heat of Neutralization of Sodium Hydroxide with Hydrochloric Acid**.** *J. Am Chem, Soc. 62 (1940) 3230-3232.*

Authors' information

[1] Research Group on Porous Solid and Calorimetry, Department of Chemistry, Faculty of Sciences, Universidad de Los Andes (Colombia), Carrera 1 No. 18 A 10,Bogotá, Colombia. Tel.:+571-3394949; E-Mail: vgarcia@uniandes.edu.co

[1*] Universidad de Los Andes, Departamento de Química, Grupo de Investigación en Sólidos Porosos y Calorimetría. Facultad de Ciencias. Author correspondence.

Juan Carlos Moreno-Piraján., Birth in Bogotá Colombia, 27 April 1964. Chemist and PhD in Chemistry received of Universidad Nacional de Colombia. I am research in the development of porous materials between others activated carbon, zeolites, clays, etc. In addition develops equipments for Calorimetry and for the synthesis of materials and measures on adsorbents materials. Professional Affiliation: Full Professor in Andes University, Colombia.

[2] Department of Chemistry, Faculty of Sciences, Universidad Nacional de Colombia, Ciudad Universitaria, Carrera 30 No. 45-03, Bogotá, Colombia.Tel.:571-3165000; E-Mail: lgiraldogu@unal.edu.co

Liliana Giraldo-Gutierréz. Birth in Bogotá Colombia. Chemist and PhD in Chemistry received of Universidad Nacional de Colombia. Research in of development of materials, instrumentation Calorimetry and solutions of theory in Thermodynamic. Profesional Affiliation: Associated Professor, D.E. in Universidad Nacional de Colombia., Bogotá, Colombia.

[3] Instituto de Física Aplicada (INFAP), CONICET-, Ejercito de Los Andes 950, Universidad Nacional de San Luis, San Luis, Argentina.+5412652430224; E-Mail: sapag@usnl.edu.ar

* Author to whom correspondence should be addressed. E-Mail: jumoreno@uniandes.edu.co